NASA
Technical
Paper
2259

January 1984

Fluid Shielding of High-Velocity Jet Noise

Jack H. Goodykoontz

NASA

NASA
Technical
Paper
2259

1984

Fluid Shielding of High-Velocity Jet Noise

Jack H. Goodykoontz

Lewis Research Center
Cleveland, Ohio

NASA
National Aeronautics
and Space Administration

**Scientific and Technical
Information Office**

1984

Summary

Experimental noise data for a nozzle exhaust system incorporating a thermal acoustic shield (TAS) are presented to show the effect of changes in geometric and flow parameters on attenuation of high-velocity jet exhaust noise in the flyover plane. The results are presented for a 10.00-cm-diameter primary conical nozzle with a TAS configuration consisting of a 2.59- or 5.07-cm-wide annular gap. Shield exhaust velocity was varied from 157 to 248 m/sec to investigate the effect of the ratio of shield-stream velocity to primary-nozzle jet velocity.

Comparing spectral data at the same ideal thrust levels showed that increasing the TAS gap width increased the attenuation of high-frequency noise. Varying the velocity ratio had a minor effect on the noise characteristics of the nozzles over the range investigated, 0.27 to 0.43. Comparing TAS noise levels with those for a coaxial nozzle at the same thrust showed that, for the small-gap nozzle, the TAS configuration had higher sound pressure levels in the forward quadrant. In the rear quadrant the sound pressure levels were approximately the same for the two configurations. For the large-gap nozzles the TAS configuration, again, had higher sound pressure levels in the forward quadrant but significantly lower levels at aft positions. Comparing TAS noise data with results predicted for a conical nozzle alone operating at the same primary-nozzle total temperature and pressure and total flow rate showed that the TAS configuration was considerably quieter but had lower ideal thrust. Conversely, on an equal-thrust basis, comparisons showed little, if any, noise reduction for the TAS configuration with the conical nozzle. This implies that a suppressor nozzle (high frequency dominated) should be used in the primary propulsion stream.

Introduction

The work presented herein is a continuation of an experimental effort, first reported in reference 1, to investigate a concept for attenuation of jet exhaust noise. The concept, a thermal acoustic shield (TAS), consists of a low-velocity, heated gas stream partially surrounding a central, or main, propulsion stream nozzle. The TAS appears to be applicable to advanced supersonic cruise civil aircraft employing inverted-velocity-profile nozzles with outer stream suppressors (refs. 2 to 4). Other recent experimental work (refs. 5 to 7) shows that jet noise was reduced when acoustic shields of various types were used. Analytical efforts have been employed in references 8 to 10 in order to understand or predict the effects of the shielding mechanism. The noise reduction is believed to be caused by reflection, refraction, noise source alteration, or a combination of all three mechanisms.

Previous results of this program (ref. 1) indicate considerable high-frequency noise reductions with the TAS configuration as compared with the noise levels of the main, or primary, nozzle flowing alone. Also reported was the insensitivity of far-field noise levels to changes in the temperature of the shield stream. The work of reference 1 was considered exploratory since only a limited range of flow conditions with one nozzle/shield configuration was investigated.

This report presents noise measurements for a TAS configuration over a more extended range of flow conditions (primarily for the shield stream) and shows the effect of varying the thickness of the shield stream. Also, the results are presented for a more efficiently designed shield-stream blocking plate (less leakage flow). TAS data are compared with those from a coaxial nozzle (blocking plates removed) and with predicted noise results for a conical nozzle. The results are compared on the basis of the same ideal thrust, in order to compare the noise reduction benefits of different configurations for comparable performance characteristics. (Other performance parameters include mass flow rate, total enthalpy change, and exit area, ref. 11.)

Results are presented for a 10.00-cm-diameter primary conical nozzle with annular flow passage (gap) widths of 2.59 and 5.07 cm. The bulk of the data are presented for a supersonic nozzle exhaust velocity ($\sim$580 m/sec) with several examples of data for a subsonic velocity (500 m/sec). Shield-stream exhaust velocity was varied from 157 to 248 m/sec, with temperatures varying from 339 to 937 K. Noise measurements are presented in terms of model-scale 1/3-octave-band sound pressure levels at various directivity angles.

Apparatus and Procedure

Facility

The flow facility used for the acoustic experiments is shown in figure 1. A common unheated laboratory air source supplied flow for two parallel flow lines: one line for the inner nozzle, and the other for the outer shield-stream flow nozzle. Each flow line had its own airflow and fuel flow control and flow-measuring systems. The air in each line could be heated by jet engine combustors. Mufflers in each line attenuated flow-control valve noise and combustion noise. The system was designed for maximum nozzle exhaust temperatures of 1100 K and nozzle pressure ratios of 3.0 in both the inner and outer streams.

A sideline microphone array, simulating the flyover plane, was used for the tests described herein. The microphones (0.635 cm diam) were placed at a constant 5.0-m distance from and parallel to the nozzle axis, as

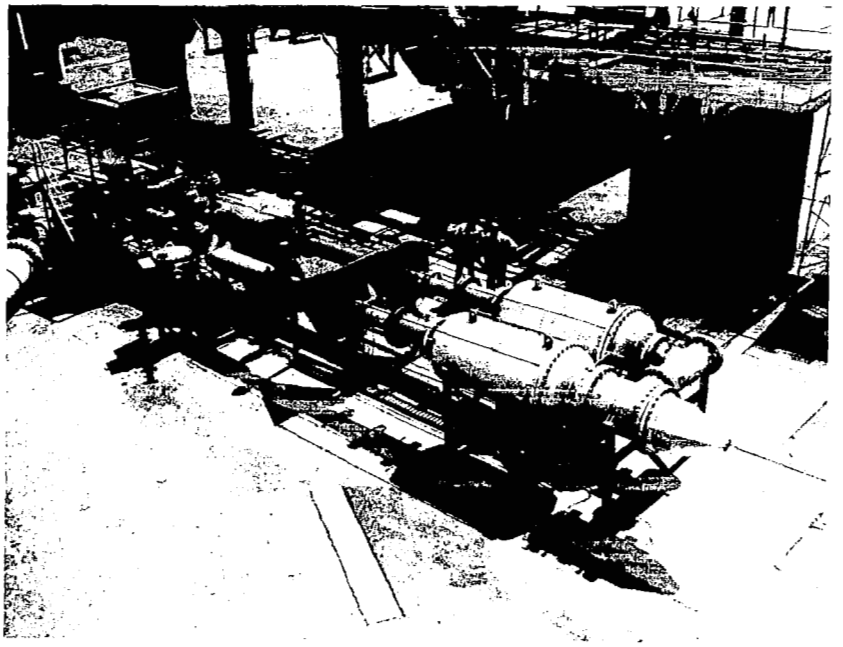

Figure 1. – Lewis hot-jet acoustic facility.

shown in figure 2. The origin of the actual jet noise angles a is the center of the nozzle exit plane. The origins of the effective jet noise angles, also tabulated in figure 2, are at different axial locations that are based on an assumed jet mixing noise distribution (ref. 12). The microphone grids were removed to improve high-frequency performance. The ground plane of the test area was asphalt and concrete and was covered with 15.25-cm-thick foam rubber pads to attenuate reflections.

Microphone	Directivity angle, θ, deg	Distance from center of nozzle exit plane to microphone, R, m	Effective jet noise angle, deg
1	46	6.93	45
2	68	5.39	65
3	95	5.02	90
4	115	5.51	110
5	129	6.48	125
6	139	7.60	135
7	148	9.39	145

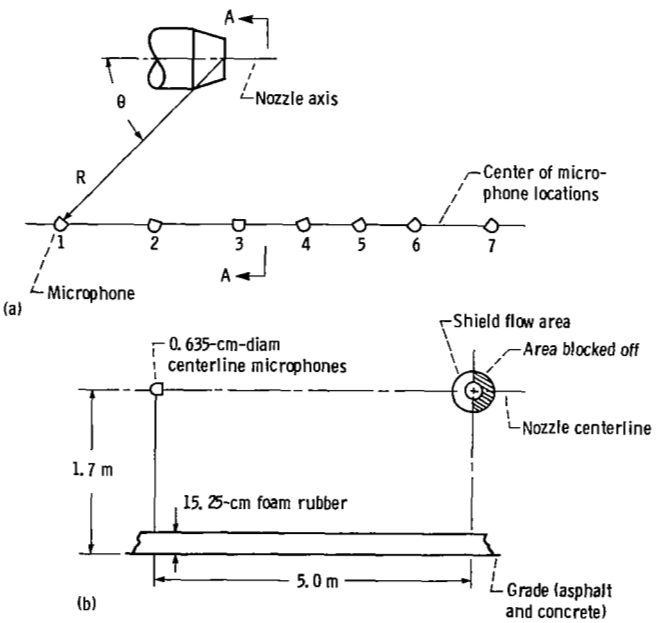

(a) Plan view.
(b) Elevation, view A-A.

Figure 2. – Schematic of flyover microphone layout.

Test Nozzles

A schematic of the test nozzle configurations is shown in figure 3. Existing coplanar coaxial nozzles (ref. 13) were modified to serve as the experimental models for the thermal acoustic shield tests. The core or conical nozzle was common to both configurations and had an inner diameter of 10.00 cm. The small-gap nozzle configuration had a gap width of 2.59 cm, and the large-gap nozzle configuration had a gap width of 5.07 cm. Two semicircular steel rings were incorporated to block one-half of the outer stream flow passage, as shown in the detail view in figure 3. The outer ring was fastened to the wall of the outer nozzle, and the inner ring was fastened to the wall of the inner nozzle. A radial clearance between the two rings allowed unobstructed axial movement between the two flow lines as a result of differential thermal expansion. The outer wall of the inner nozzle was coated with a ceramic material to minimize heat transfer between the two streams during operation. The interior of the upstream portion of the inner nozzle supply line was also lined with insulating material.

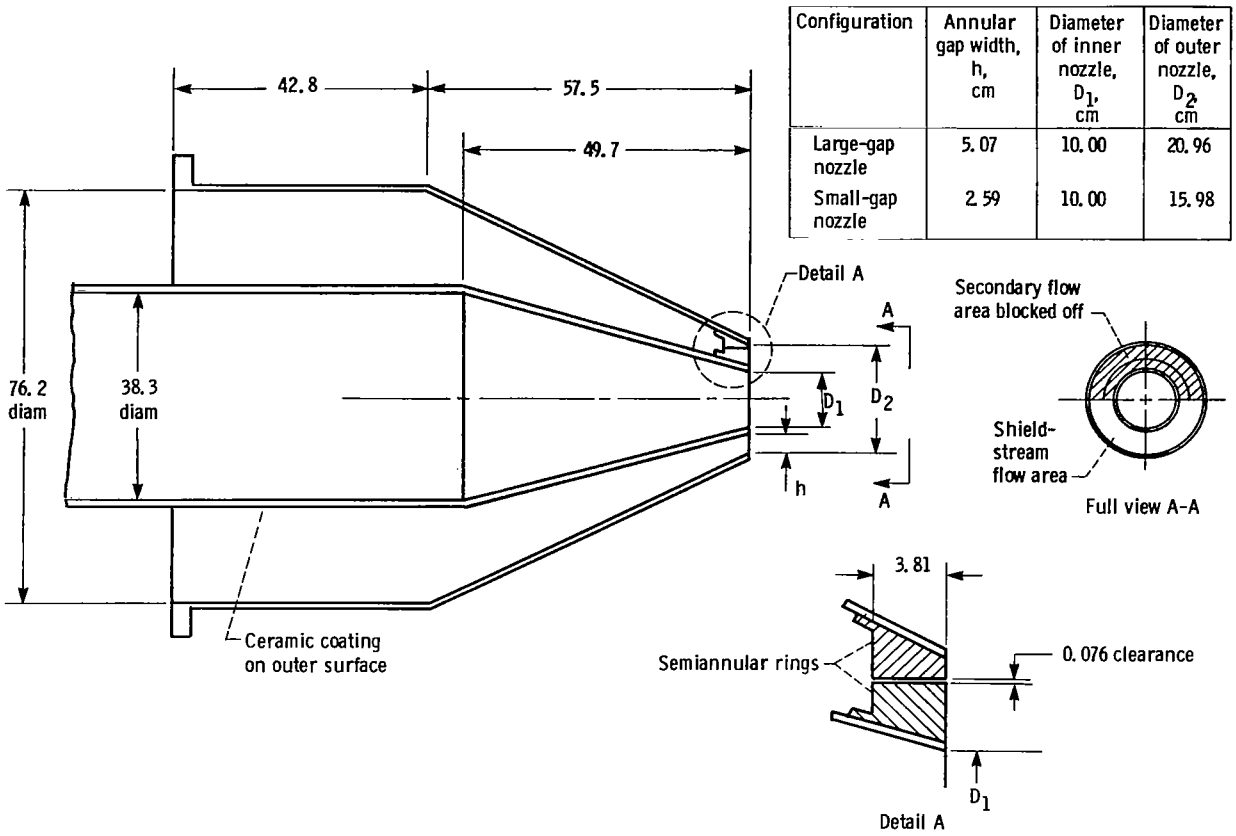

Configuration	Annular gap width, h, cm	Diameter of inner nozzle, D_1, cm	Diameter of outer nozzle, D_2, cm
Large-gap nozzle	5.07	10.00	20.96
Small-gap nozzle	2.59	10.00	15.98

Figure 3. – Schematic of thermal acoustic shield nozzle configurations. (All dimensions are in centimeters.)

Procedure

All tests were conducted with steady-state flow conditions for given nozzle total pressures and temperatures. Upstream plenum chamber total pressures and total temperatures were used to calculate nozzle exhaust velocities by assuming ideal expansion to atmospheric conditions. Total temperatures were corrected for thermocouple radiation heat loss.

An on-line analysis of the noise signal from each microphone in succession was performed. One-third-octave-band sound presure level spectra were digitally recorded and subsequently processed to give lossless data at the particular microphone location. Lossless data were obtained by adding atmospheric attenuation (ref. 14) to the spectral data. It was determined that the spectral data above 1000 Hz were free field (free from ground reflections) by comparing them with the free-field data reported in reference 13 for flow from the conical nozzle alone.

Predicted conical-nozzle-alone spectra were calculated from the equations and methods outlined in appendix A. The equations were taken from reference 12 and were simplified to give spectra for a single-stream conical nozzle in a static environment. The method of calculating ideal thrust for the TAS configurations is also given in appendix A. All symbols are defined in appendix B.

Results and Discussion

Data are presented here that compare the current experimental results with those obtained previously (ref. 1). Then noise data are compared to show the effect of changes in cycle conditions (pressure and temperature), including the variation of shield-stream total temperature and velocity ratio. Next, various nozzle configurations are compared to show the effect of geometry changes, including variation in shield-stream gap width; semi-annular flow (TAS) versus full-annular flow (coaxial nozzle); and finally, TAS results versus predicted results for a conical nozzle alone (without shield-stream flow).

Comparison of Current and Previous Experimental Results

One of the objectives of the current experimental program was to obtain thermal acoustic shield data by using a blocking-plate design having less leakage flow in

the shield-stream passage than the design used in the previous program (ref. 1). It was felt that the previous data may not be representative of a semiannular flow configuration as a result of the relatively large leakage flow through the blocked-off area.

The current acoustic data are compared with data from reference 1 for a subsonic primary-nozzle (conical) flow condition in figure 4. Noise data are compared at three directivity angles for flow from the conical nozzle alone (for reference purposes) and from the 2.59-cm-gap-width shield-stream flow configuration. The agreement of the data for the conical nozzle flow alone is good at all three angles and at all frequencies except at very low frequencies (<400 Hz, where ground reflections may appear). The shield-stream flow results for the two tests at directivity angles of 46° (fig. 4(a)) and 95° (fig. 4(b)) are essentially the same at frequencies greater than 400 Hz. (Below 400 Hz, differences are attributed to anomalies related to ground reflection phenomena.) At a directivity angle of 129° (fig. 4(c)) the current shield configuration data are slightly below those of the previous experiments in the middle-frequency range (2000 to 16 000 Hz). The results for the remainder of the spectrum are in agreement for the two sets of shield-stream flow data.

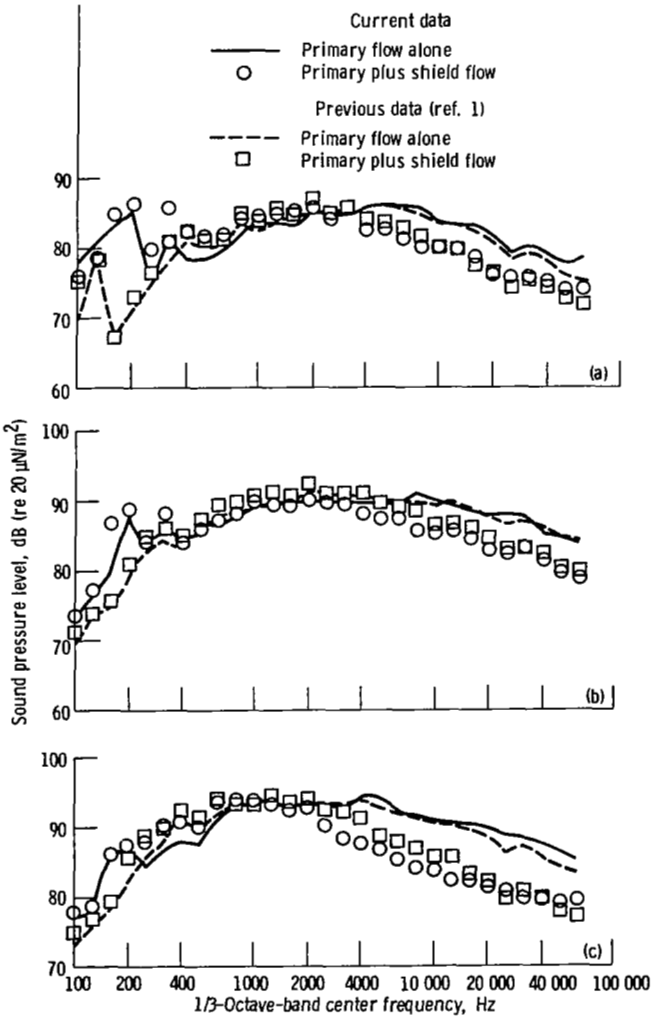

(a) $\theta = 46°$.
(b) $\theta = 95°$.
(c) $\theta = 129°$.

Figure 4. – Comparison of current acoustic data with data from reference 1 for subsonic primary flow conditions at different directivity angles θ. Nominal primary-nozzle flow conditions: pressure ratio, PR_j, 1.8; total temperature, T_j, 289 K; velocity, V_j, 300 m/sec; Mach number, M_j, 0.950. Nominal shield-stream flow conditions: velocity, V_s, 220 m/sec; total temperature, T_s, 956 K. Gap width, 2.59 cm.

Shield-stream flow data (gap width, 2.59 cm) for a supersonic primary-nozzle flow condition are compared with data from reference 1 in figure 5. Conical-nozzle-alone data were not available for comparison at this flow condition. At directivity angles of 46° (fig. 5(a)) and 95° (fig. 5(b)) the data are in good agreement over the entire frequency range. At 129° (fig. 5(c)) a slight disagreement between the two sets of data exists in the rear quadrant at frequencies greater than 6300 Hz, with the current data being below the previous data.

It is felt that the differences in shield-stream flow rates encountered in the two tests had a minor effect on the noise characteristics of the thermal acoustic shield configuration, either for subsonic or supersonic primary-nozzle flow conditions. Therefore the trends noted in reference 1 are believed to be valid for a semiannular thermal acoustic shield configuration.

Effect of Cycle Changes on Noise Characteristics of TAS Configurations

Variation in shield temperature. – The effect of shield-stream total temperature on the sound pressure level spectra for the 2.59-cm-gap-width TAS nozzle configuration is shown in figure 6. The data are presented for a supersonic primary-nozzle flow condition with the shield-stream temperature varying from slightly above ambient (339 K) to the maximum allowable temperature of the facility (964 K for the shield stream at the given flow rate). Data from reference 1 are included for an intermediate-temperature case (713 K). The ratio of shield-stream ideal exhaust velocity V_s to primary-nozzle ideal exhaust velocity V_j is approximately the same for the temperature conditions shown. Weight flow ratio, also tabulated in the figure, varied by a factor of 2.3 with total ideal thrust levels varying by about 13 percent. The noise data were not corrected for this difference.

At directivity angles of 46° and 95° (figs. 6(a) and (b), respectively) the sound pressure levels for the unheated-flow condition (339 K) are slightly greater than those for the heated-flow conditions at frequencies greater than 4000 Hz. Also, at 95° (fig. 6(b)) the levels for the hottest flow condition (964 K) are the lowest at frequencies from 2000 to 16 000 Hz. This reduction of sound pressure

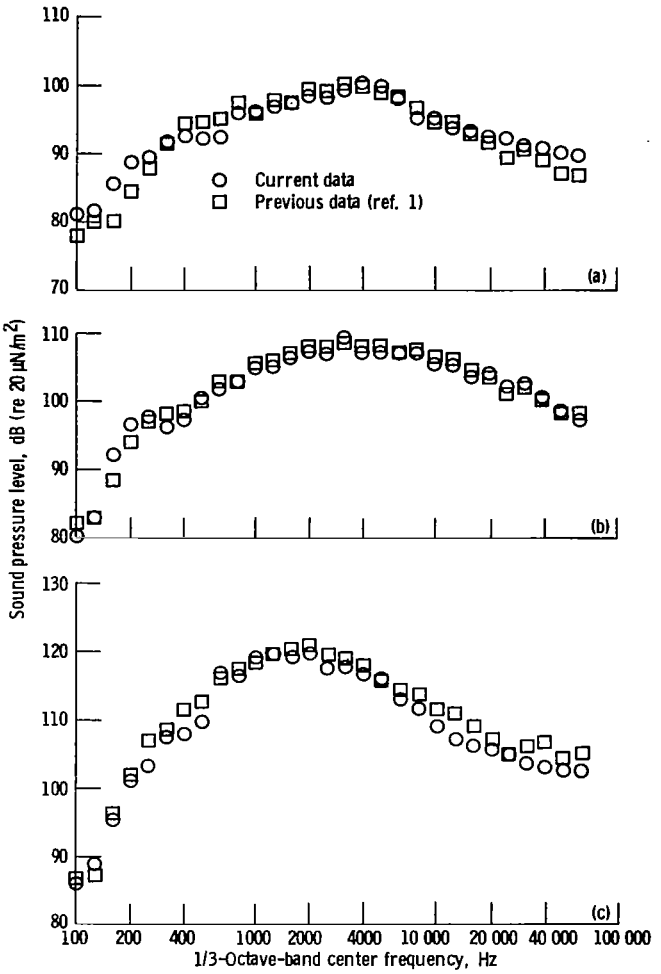

(a) $\theta = 46°$.
(b) $\theta = 95°$.
(c) $\theta = 129°$.

Figure 5. – Comparison of current acoustic data with data from reference 1 for supersonic primary flow conditions at different directivity angles θ. Nominal primary-nozzle flow conditions: pressure ratio, PR_j, 2.17; total temperature, T_j, 1089 K; velocity, V_j, 667 m/sec; Mach number, M_j, 1.14. Nominal shield-stream flow conditions: velocity, V_s, 218 m/sec; total temperature, T_s, 945 K. Gap width, 2.59 cm.

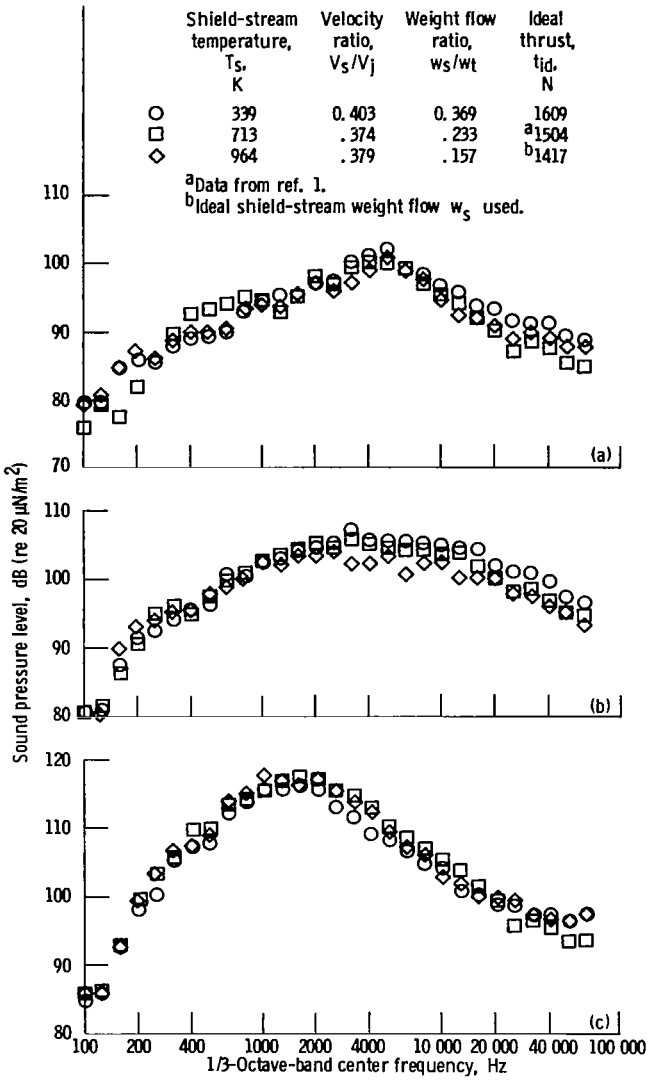

(a) $\theta = 46°$.
(b) $\theta = 95°$.
(c) $\theta = 129°$.

Figure 6. – Effect of shield-stream temperature on sound pressure level spectra for 2.59-cm-gap-width thermal acoustic shield configurations at supersonic primary-nozzle flow conditions and different directivity angles θ. Nominal primary-nozzle flow conditions: pressure ratio, PR_j, 2.19; total temperature, T_j, 816 K; velocity, V_j, 581 m/sec.

levels with increasing shield-stream temperature is qualitatively consistent with acoustic shielding theory (ref. 15). However, at 129° (fig. 6(c)) the sound pressure levels are approximately the same for all flow conditions over the entire frequency range (except for frequencies greater than 25 kHz, where anomalous behavior occurs).

Data for the 5.07-cm-gap-width TAS configuration are shown in figure 7 for two conditions of heated shield-stream flow and a supersonic primary-nozzle flow. Unheated-flow data are not available for the nozzle configuration. The velocity ratio for the two cases is the same, with weight flow ratio varying by approximately 41 percent and ideal thrust levels varying by about 3 percent. The sound pressure levels at all directivity angles are approximately the same for the two shield-stream temperatures shown.

From the results of figures 6 and 7 it appears that shield-stream temperature has only a slight effect on the noise radiation characteristics of a TAS nozzle configuration, at least when a simple conical nozzle is used in the primary propulsion stream. This agrees with the conclusions of reference 1.

Variation of velocity ratio. – Reference 1 concluded that for a TAS configuration, attenuation (relative to the

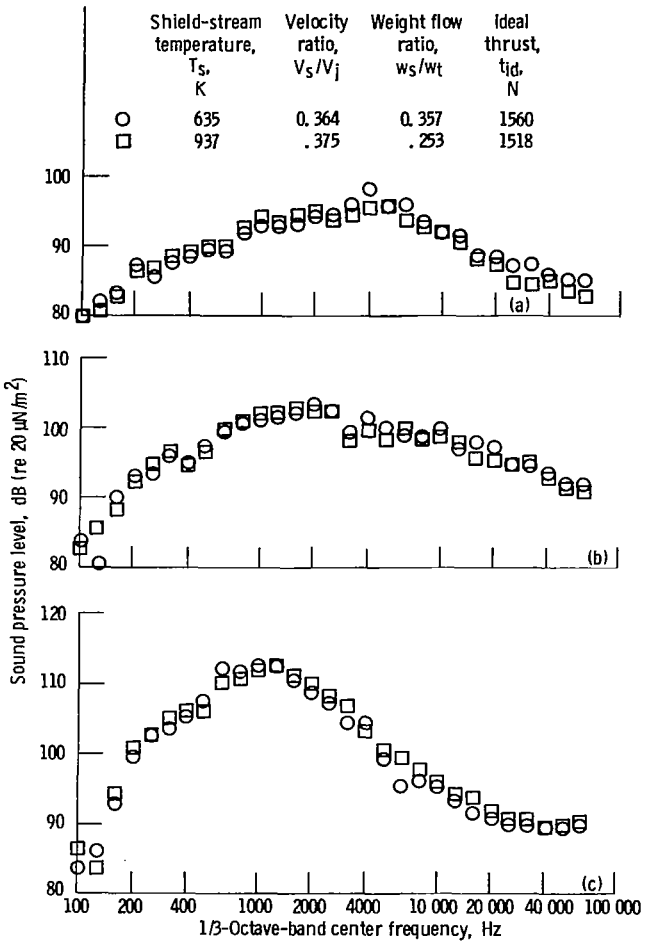

(a) $\theta = 46°$.
(b) $\theta = 95°$.
(c) $\theta = 129°$.

Figure 7. – Effect of shield-stream temperature on sound pressure level spectra for 5.07-cm-gap-width thermal acoustic shield configurations at supersonic primary-nozzle flow conditions and different directivity angles θ. Nominal primary-nozzle flow conditions: pressure ratio, PR_j, 2.21; total temperature, T_j, 814 K; velocity, V_j, 582 m/sec.

isolated primary nozzle) increased with a decrease in the ratio of shield-stream to primary-nozzle ideal exhaust velocity. Velocity ratios were varied in reference 1 by merely changing the primary-nozzle exhaust velocity while holding the shield-stream velocity constant. This section presents results with velocity ratio varied by changing the shield-stream velocity (at constant temperature) and holding the primary-nozzle exhaust velocity constant.

Results for supersonic flow from the primary nozzle for the 2.59-cm-gap-width TAS configuration are shown in figure 8. The results are presented as measured; that is, no attempt was made to correct for differences in thrust levels (changes in the results would be minimal). Data from reference 1 for a velocity ratio of 0.37 are also included for comparison.

At directivity angles of 46° (fig. 8(a)) and 95° (fig. 8(b)) the four sets of data show about the same values of sound pressure level over the entire frequency range. At 129° (fig. 8(c)) the data start to diverge at frequencies greater than 1000 Hz. However, the results are inconsistent and in direct opposition to the conclusions of reference 1. Except for the 0.31-velocity-ratio data the high-frequency (>10 kHz) sound pressure levels appear to decrease slightly with increasing velocity ratio. Similar results were obtained for a subsonic primary-nozzle flow condition (not shown) with even less effect of velocity ratio on the high-frequency sound pressure levels.

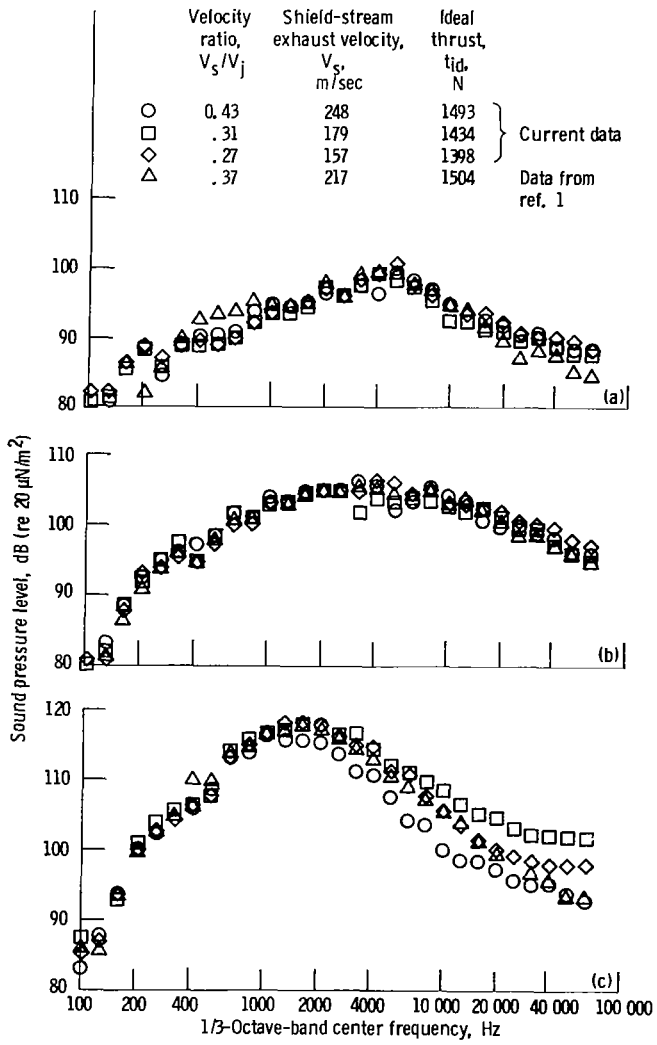

(a) $\theta = 46°$.
(b) $\theta = 95°$.
(c) $\theta = 129°$.

Figure 8. – Effect of velocity ratio on sound pressure level spectra for 2.59-cm-gap-width thermal acoustic shield configurations at supersonic primary-nozzle flow conditions and different directivity angles θ. Nominal primary-nozzle flow conditions: pressure ratio, PR_j, 2.22; total temperature, T_j, 814 K; velocity, V_j, 583 m/sec. Nominal shield-stream total temperature, T_s, 709 K.

The effect of velocity ratio variation on sound pressure levels for the 5.07-cm-gap-width TAS configuration is shown in figure 9 for a supersonic primary-nozzle flow condition. For this configuration the effect of changing velocity ratio is negligible at all angles shown. Similar results were obtained for a subsonic primary flow. A comparison of figures 8(c) and 9(c) implies that the effect (if any) of velocity ratio variation is larger for the narrower-gapped TAS configurations. It is concluded that the effects of variation in velocity ratio, over the 0.27 to 0.43 range investigated, on the noise characteristics of a TAS system are minimal.

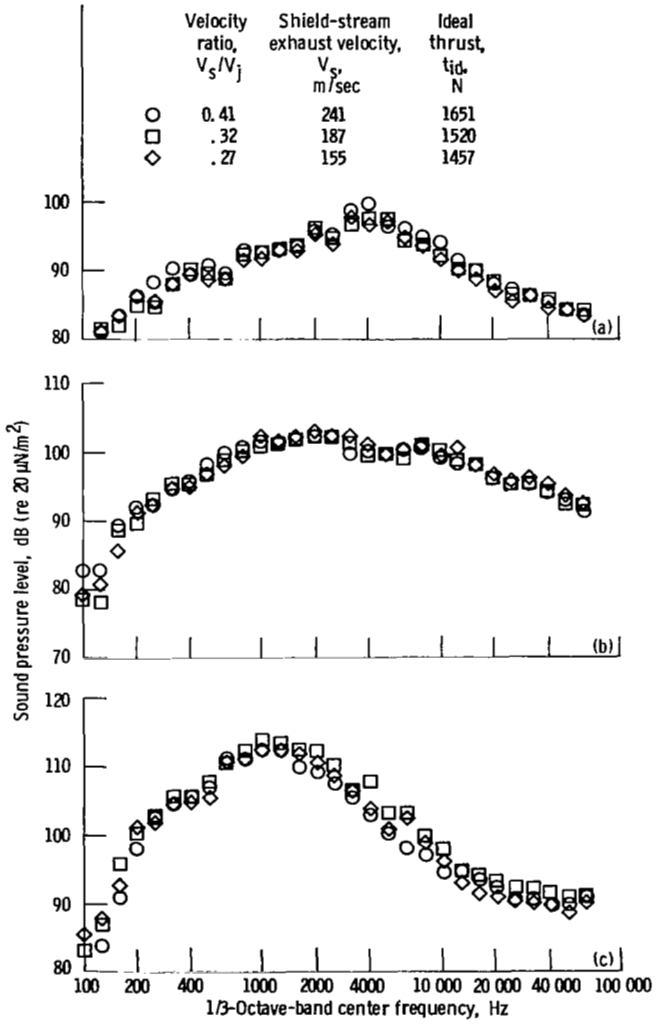

(a) $\theta = 46°$.
(b) $\theta = 95°$.
(c) $\theta = 129°$.

Figure 9. – Effect of velocity ratio on sound pressure level spectra for 5.07-cm-gap-width thermal acoustic shield configurations at supersonic primary-nozzle flow conditions and different directivity angles θ. Nominal primary-nozzle flow conditions: pressure ratio, PR_j, 2.21; total temperature, T_j, 812 K; velocity, V_j, 581 m/sec. Nominal shield-stream total temperature, T_s, 698 K.

Comparison of Noise Characteristics of Various Nozzle Configurations

Effect of variation in gap width for a TAS configuration. – Noise data for two TAS configurations with different gap widths and the same values of ideal thrust are compared in figure 10 for supersonic primary-nozzle flow. The primary-flow-stream nozzle was operated at the same pressure and temperature for both cases. The shield-stream total pressures and temperatures were adjusted so that shield-stream velocity and flow rate were approximately the same for both nozzle configurations. It was shown previously that variation in shield-stream temperature has only a slight effect on the far-field noise levels for the TAS configurations tested in this program. It is clear from the data shown in figure 10 that the larger-gap nozzle (5.07 cm) has lower high-frequency sound pressure levels (4 to 9 dB) and that the difference increases with increasing directivity angle.

Data for subsonic primary-nozzle flow are shown in figure 11. The trends are similar to the supersonic flow condition. The differences in high-frequency levels at 46° (fig. 11(a)) and 95° (fig. 11(b)) are about the same as those for the supersonic flow condition. However, at 129° (fig. 11(c)) the difference in high-frequency levels (2 dB) is considerably less than was found for supersonic primary flow (9 dB).

Comparison of TAS and coaxial nozzle data. – Noise data for the small-semiannular-gap TAS configuration and the coaxial nozzle at about equal thrust levels are compared in figure 12 for supersonic primary flow. The coaxial nozzle arrangement was attained by removing the blocking plates (fig. 3) from the secondary (or shield stream) flow passage. A coaxial nozzle may also be considered a TAS configuration but with full annular flow. The thrust levels of the two sets of TAS data in figure 12 bracket the coaxial-nozzle thrust levels by approximately ±5 percent. Shield-stream velocity is the same for all cases, and temperatures are the same for two out of the three sets.

At a directivity angle of 46° (fig. 12(a)) the sound pressure levels are the same at frequencies less than 2500 Hz. Above this frequency the levels for the TAS configurations are greater than those for the coaxial nozzle. At 95° (fig. 12(b)) the differences in the high-frequency levels (>2500 Hz) are less; however, it still appears that the levels for the TAS configurations may be greater in the high-frequency range. At 129° (fig. 12(c)) the three configurations have approximately the same sound pressure levels over the entire frequency range (except above 40 kHz). Similar results were obtained for a subsonic primary-nozzle flow condition.

Results for the 5.07-cm-gap-width nozzle, for supersonic primary-nozzle flow, are shown in figure 13. The ideal thrust levels are within 3.5 percent for the two sets of data shown, with shield-stream temperatures

Configuration	Primary nozzle				Shield stream				Ideal thrust, t_{id}, N
	Pressure ratio, PR_j	Total temperature T_j, K	Velocity V_j, m/sec	Weight flow, w_j, kg/sec	Pressure ratio, PR_s	Total temperature, T_s, K	Velocity, V_s, m/sec	Weight flow, w_s, kg/sec	
○ 2.59-cm-gap-width nozzle	2.17	826	580	2.30	1.34	339	234	1.35	1650
□ 5.07-cm-gap-width nozzle	2.21	819	584	2.36	1.13	635	213	1.27	1646

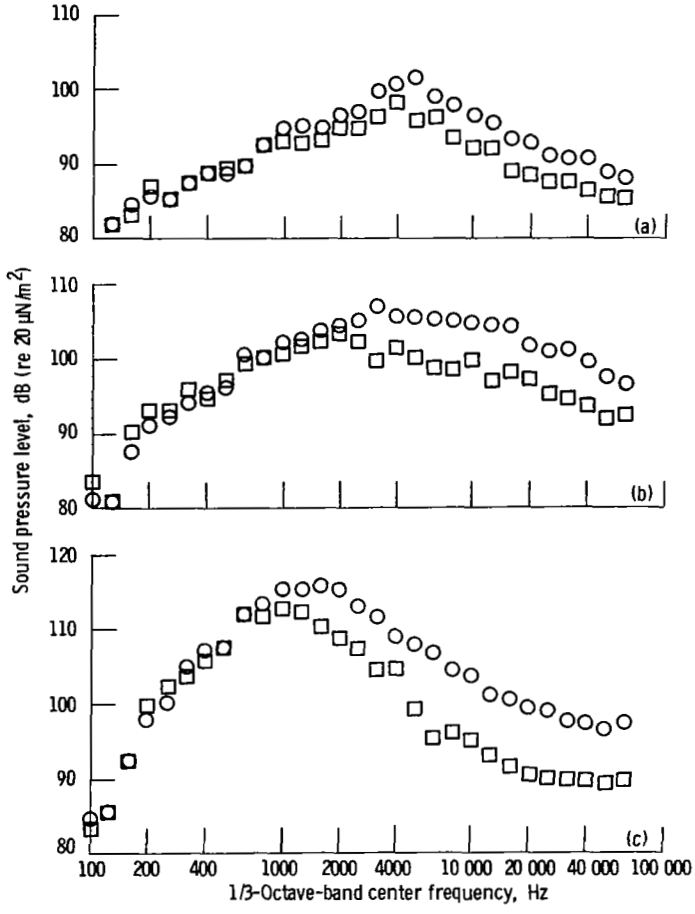

(a) $\theta = 46°$.
(b) $\theta = 95°$.
(c) $\theta = 129°$.

Figure 10. – Effect of gap width on noise data for thermal acoustic shield configurations at equal thrust levels and different directivity angles θ—supersonic primary-nozzle flow.

Configuration	Primary nozzle				Shield stream				Ideal thrust, t_{id}, N
	Pressure ratio, PR_j	Total temperature T_j, K	Velocity V_j, m/sec	Weight flow, w_j, kg/sec	Pressure ratio, PR_s	Total temperature, T_s, K	Velocity, V_s, m/sec	Weight flow, w_s, kg/sec	
○ 2.59-cm-gap-width nozzle	1.82	825	514	1.82	1.35	304	224	1.46	1267
□ 5.07-cm-gap-width nozzle	1.74	816	493	1.88	1.14	633	214	1.26	1197

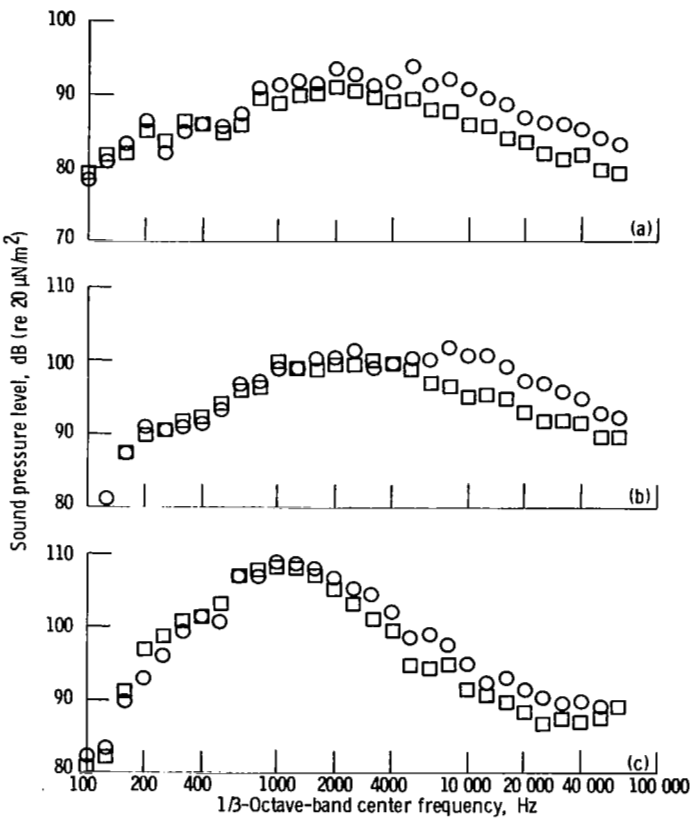

(a) $\theta = 46°$.
(b) $\theta = 95°$.
(c) $\theta = 129°$.

Figure 11. – Effect of gap width on noise data for thermal acoustic shield configurations at equal thrust levels and different directivity angles θ—subsonic primary-nozzle flow.

Configuration		Primary nozzle				Shield stream				Ideal thrust, t_{id}, N
		Pressure ratio, PR_j	Total temperature T_j, K	Velocity V_j, m/sec	Weight flow, w_j, kg/sec	Pressure ratio, PR_s	Total temperature, T_s, K	Velocity, V_s, m/sec	Weight flow, w_s, kg/sec	
○	Coaxial nozzle	2.20	816	582	2.30	1.16	708	241	0.94	1566
□	TAS nozzle	2.17	826	580	2.30	1.34	339	234	1.35	1650
◇	TAS nozzle	2.21	813	581	2.36	1.16	716	248	.49	1490

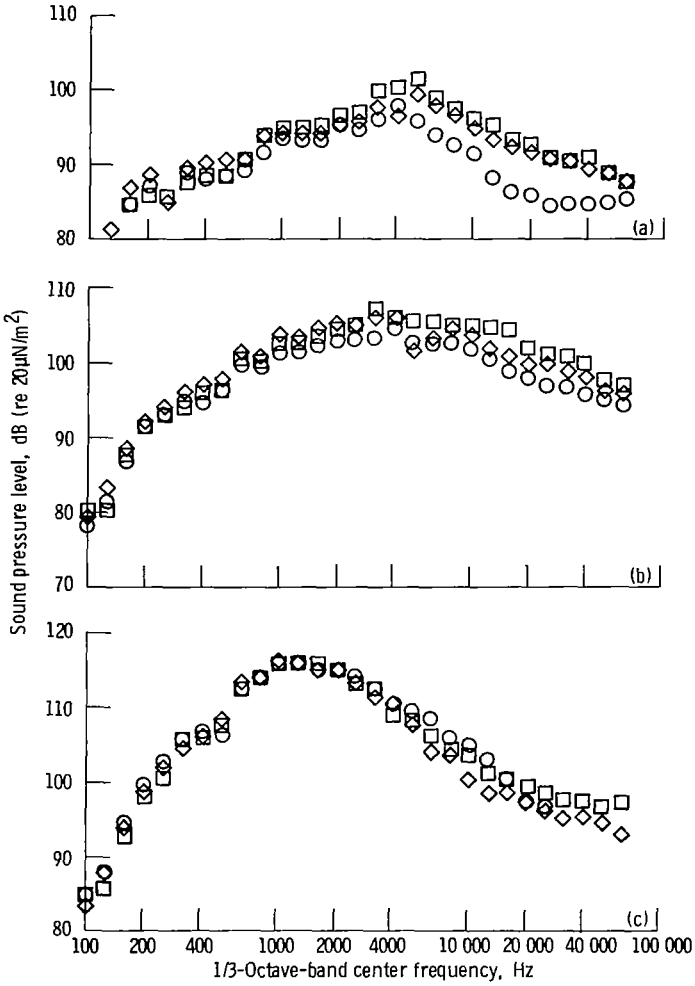

(a) $\theta = 46°$.
(b) $\theta = 95°$.
(c) $\theta = 129°$.

Figure 12. – Comparison of thermal acoustic shield configuration and coaxial nozzle noise data at equal thrust levels and different directivity angles θ—2.59-cm-gap-width nozzle. Supersonic primary nozzle flow.

Configuration	Primary nozzle				Shield stream				Ideal thrust, t_{id}, N
	Pressure ratio, PR_j	Total temperature T_j, K	Velocity V_j, m/sec	Weight flow, w_j, kg/sec	Pressure ratio, PR_s	Total temperature, T_s, K	Velocity, V_s, m/sec	Weight flow, w_s, kg/sec	
○ Coaxial nozzle	2.21	816	582	2.40	1.06	702	155	1.57	1637
□ TAS nozzle	2.22	812	582	2.40	1.16	696	241	1.27	1695

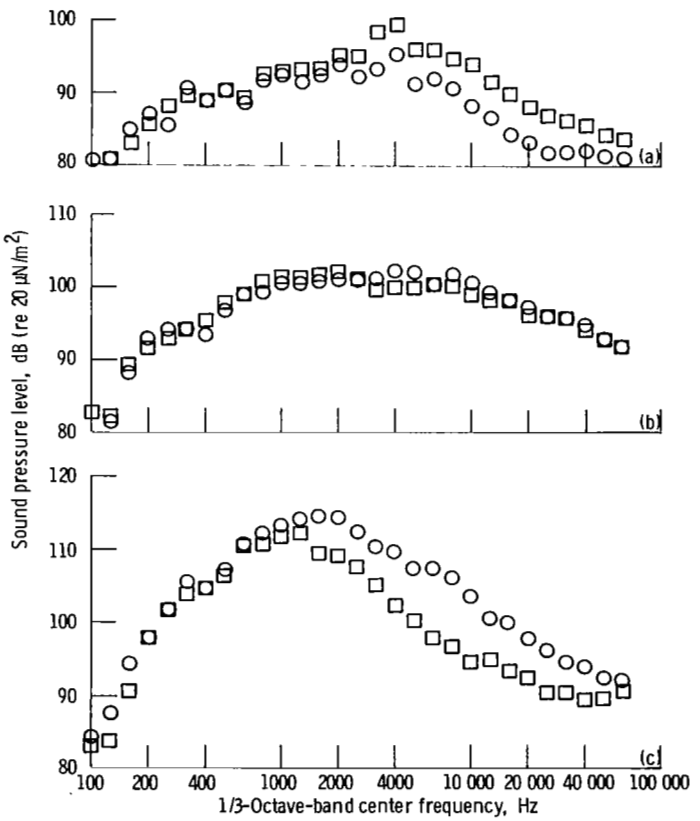

(a) $\theta = 46°$.
(b) $\theta = 95°$.
(c) $\theta = 129°$.

Figure 13. – Comparison of thermal acoustic shield and coaxial nozzle noise data at equal thrust levels and different directivity angles θ—5.07-cm-gap-width nozzle. Supersonic primary-nozzle flow.

approximately the same but at different shield-stream velocities. At 46° (fig. 13(a)) the TAS configuration, again, has higher sound pressure levels at frequencies greater than 2500 Hz. At 95° (fig. 13(b)) the two sets of data are the same over the entire spectrum. At 129° (fig. 13(c)) the levels for the TAS configuration are considerably below those for the coaxial nozzle at frequencies greater than 2500 Hz. Similar results were obtained for subsonic primary-nozzle flow.

Comparison of TAS noise data with conical nozzle prediction. – In reference 1 data are presented to indicate the noise reduction benefit of the TAS configuration by merely comparing the results for the conical nozzle alone (without shield flow) and the conical nozzle with shield flow. In this case the total ideal thrust of the TAS configuration ranged from 8 to 20 percent greater than that for the conical nozzle alone (based on ideal flow conditions). The increase in thrust level is a result of having two independently controlled flow streams available for the experimental work.

A practical application of the TAS system to an aircraft engine would possibly require that the shield stream be bled from the flow forming the primary propulsive stream (ref. 5). As a result of the bleed flow the engine equipped with a TAS system would have less ideal thrust than an engine using a nozzle without the TAS for the same pressures and temperatures in the main propulsion stream and the same total flow rate. The reduction in ideal thrust would be a function of the fraction of flow bled off and the velocity of the shield stream.

It is desirable to determine the trade-off between noise reduction and thrust loss due to incorporation of a TAS system. Therefore this section compares experimental noise data for a TAS configuration with predicted noise results for a conical nozzle alone (without TAS).

Small-gap TAS configuration spectral data are compared with predictions (ref. 12) for a simple conical nozzle in figure 14 for a directivity angle of 129°. Two conical nozzle predicted spectra are shown as indicated by the curves in the figure. The solid curve represents the spectra for a conical nozzle operating at the same cycle conditions (pressure and temperature) as the primary nozzle of the TAS configuration and at the same total flow. The dashed curve represents predicted results for a conical nozzle operating at the same temperature and velocity as the mixed values for the TAS configuration and consequently at the same ideal thrust levels. (Ideal flow rate in the shield stream is used for the TAS nozzle as a result of the uncertainty in measurement of this flow.)

The TAS configuration is shown in figure 14 to have considerably lower sound pressure levels than the conical nozzle under the same cycle conditions (solid curve) at frequencies greater than 2000 Hz. Comparing the two thrust levels listed in the table indicates a difference of about 14 percent for a ratio of shield-stream flow to total flow of 22 percent. On the other hand the conical nozzle

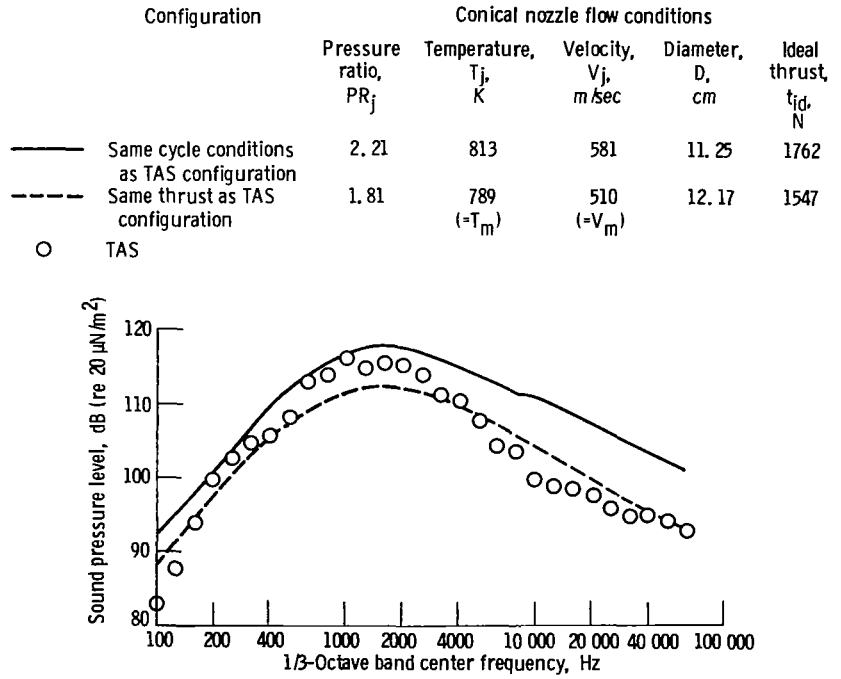

Figure 14. – Comparison of 2.59-cm-gap-width thermal acoustic shield configuration noise data with predicted conical nozzle results (ref. 12). Directivity angle, θ, 129°. TAS primary-nozzle flow conditions: pressure ratio, PR_j, 2.21; total temperature, T_j, 813 K; velocity, V_j, 581 m/sec. TAS shield-stream flow conditions: temperature, T_s, 715 K; velocity, V_s, 248 m/sec; weight flow ratio, w_s/w_t, 0.222.

predicted spectrum for the same mixed flow properties (equal thrust) agrees somewhat with the TAS data, although there may be a slight increase in middle-frequency noise and a slight reduction in high-frequency noise for the TAS.

Similar calculations were made for the 5.07-cm-gap-width TAS configuration and the results are presented in figure 15. For this case the difference in sound pressure level between the TAS configuration and the conical nozzle with the same cycle conditions is even greater than for the small-gap nozzle. However, the difference in thrust level has increased to about 20 percent as a result of the increased area and consequent increase in shield-stream flow (ratio of shield-stream flow to total flow, ~35 percent). Again the conical nozzle prediction based on the same mixed flow properties agrees fairly well with the TAS data, although for this larger-gap configuration there is a more consistent reduction in high-frequency noise for the TAS.

The results shown in figures 14 and 15 indicate that a TAS system reduces noise levels as compared with a conical nozzle operating at the same cycle conditions. Unfortunately there is an accompanying loss in ideal thrust. The net benefit (noise reduction versus economics) would have to be determined from a detailed mission analysis study. The reduction in high-frequency noise obtained with the TAS is an attractive consequence since suppressor nozzles, which are dominant in high-frequency-noise emission, are the most likely candidates for future civil supersonic cruise aircraft (ref. 16). The results obtained in this work are generally in agreement with both the experimental results of references 5 to 7 and the trends noted in the theoretical studies of references 8 to 10.

Conclusions

An experiment was conducted to determine the effect of variation in cycle conditions and geometry on the noise-generating characteristics of a thermal acoustic shield (TAS) configuration using a conical nozzle for the main propulsion stream. Results were obtained for variations in shield-stream temperature, velocity ratio, and shield-stream gap width. Also, comparisions were made with other types of nozzles (coaxial and conical). The results of the tests are summarized as follows:

1. The combination of TAS and a conical primary nozzle showed no improvement in terms of noise reduction when compared with predicted results from a conical nozzle alone operating at the same total thrust level.

2. The TAS configuration exhibited considerably lower high-frequency sound pressure levels than those predicted for a conical nozzle operating at the same cycle conditions (primary total pressure and temperature) and total flow rate as the TAS nozzle. However, the ideal thrust levels were less for the TAS configuration. The reduction in high-frequency noise suggests the use of a suppressor nozzle (high frequency dominant) in the main propulsion stream.

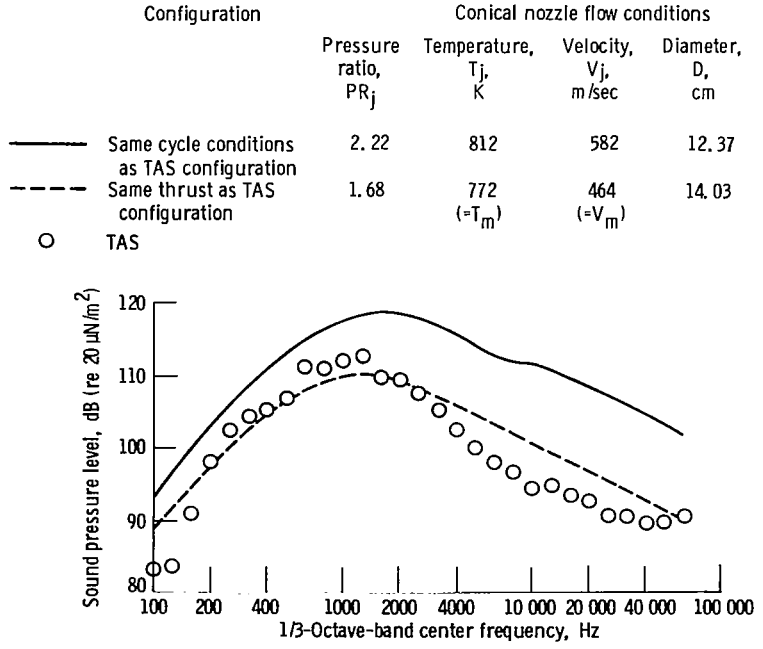

Figure 15. – Comparison of 5.07-cm-gap-width thermal acoustic shield configuration noise data with predicted conical nozzle results (ref. 12). Directivity angle, θ, 129°. TAS primary-nozzle flow conditions: pressure ratio, PR_j, 2.22; total temperature, T_j, 812 K; velocity, V_j, 582 m/sec. TAS shield-stream flow conditions: temperature, T_s, 696 K; velocity, V_s, 241 m/sec; weight flow ratio, w_s/w_t, 0.346.

3. Comparing sound pressure levels for a TAS configuration (semiannular secondary flow) and a coaxial nozzle configuration (full-annular secondary flow), at the same ideal thrust gave the following results:

a. For the small-gap secondary flow passage (2.59 cm) the TAS configuration had greater high-frequency sound pressure levels in the forward quadrant than the coaxial nozzle, but in the rear quadrant (near the peak noise location) the levels for the two configurations were the same over the entire spectrum.

b. For the large-gap secondary flow passage (5.07 cm) the TAS configuration, again, had greater high-frequency sound pressure levels in the forward quadrant but considerably lower high-frequency levels in the rear quadrant.

4. Increasing the width of the shield caused a decrease in high-frequency sound pressure levels at all directivity angles. The comparison was made for equal ideal-thrust levels.

5. For the ranges investigated, varying shield-stream temperature or velocity ratio had a minor or negligible effect on the noise-generating characteristics of a TAS nozzle configuration when a simple conical nozzle was used in the primary propulsion stream.

National Aeronautics and Space Administration
Lewis Research Center
Cleveland, Ohio, June 3, 1983

Appendix A

Methods and Equations Used to Determine Predicted Conical Nozzle Spectra and Ideal Thrust

Predicted Conical Nozzle Spectra

The output of the semiempirical prediction procedure of reference 12 is sound pressure level spectra at a particular angle. The prediction calculates the spectra for shock-free jet-mixing noise, including the effects of flight (not applicable for the work presented herein). Then supersonic jet shock-noise effects (if any) are calculated separately and added antilogarithmically to the shock-free jet-mixing spectra. The sound pressure levels are free field, far field, and lossless. The following development is for a single-stream conical nozzle in a static environment.

For the jet-mixing noise portion of the spectrum, solutions of two equations and a table entry are needed. The first equation, giving the mixing-noise frequency parameter S_n, is

$$S_n=\frac{fD}{V_j}\left(\frac{T_j}{T_a}\right)\exp\left\{0.4\left[1+\cos\theta\left(\frac{V_j}{C_a}\right)^{0.1}\right]\right\} \tag{A1}$$

Values of the logarithm of S_n are tabulated in table I.

The second equation, giving the overall sound pressure level uncorrected for refraction $\mathrm{UOL_n}$, is

$$\mathrm{UOL}_n=141+10\log\left[\left(\frac{\rho_a}{\rho_{\mathrm{ISA}}}\right)^2\left(\frac{C_a}{C_{\mathrm{ISA}}}\right)^4\right]$$
$$+10\log\left(\frac{A}{R^2}\right)+10\log\left(\frac{\rho_j}{\rho_a}\right)^{\omega}+10\log\left(\frac{V_j}{C_a}\right)^{7.5}$$
$$-15\log\left\{\left[1+0.62\left(\frac{V_j}{C_a}\right)\cos\theta\right]^2+0.015\left(\frac{V_j}{C_a}\right)^2\right\} \tag{A2}$$

where

$$\omega=\frac{3\left(\frac{V_j}{C_a}\right)^{3.5}}{0.6+\left(\frac{V_j}{C_a}\right)^{3.5}}-1 \tag{A2a}$$

Values of $(\mathrm{SPL}_n-\mathrm{UOL}_n)$ are tabulated in table I for various corrected directivity angles

$$\theta'=\theta\left(\frac{V_j}{C_a}\right)^{0.1} \tag{A2b}$$

SPL as a function of frequency for a given directivity angle is then evaluated from these expressions.

The procedure for evaluating the shock-noise component of the combined spectrum is similar in that two equations must be solved: one for a frequency parameter S_{sh}, and one for an overall sound pressure level uncorrected for refraction UOL_{sh}. Then a graph of $\mathrm{SPL}_{sh}-\mathrm{UOL}_{sh}$ as a function of the logarithm of the frequency parameter is used to obtain values of $\mathrm{SPL_{sh}}$.

The first equation, giving the frequency parameter S_{sh}, is

$$S_{sh}=\left(\frac{fD}{0.7\,V_j}\right)\times(M_j^2-1)^{1/2}$$
$$\times\left\{\left[1+0.7\left(\frac{V_j}{C_a}\right)\cos\theta\right]^2+0.019\left(\frac{V_j}{C_a}\right)^2\right\}^{1/2} \tag{A3}$$

The second equation, giving the overall sound pressure level uncorrected for refraction UOL_{sh}, is

$$\mathrm{UOL}_{sh}=162+10\log\left[\left(\frac{\rho_a}{\rho_{\mathrm{ISA}}}\right)^2\left(\frac{C_a}{C_{\mathrm{ISA}}}\right)^4\right]$$
$$+10\log\left(\frac{A}{R^2}\right)+10\log\left[\frac{(M_j^2-1)^2}{1+(M_j^2-1)^2}\right]+F(\theta-\theta_M) \tag{A4}$$

where the function F is given by

$$F=0 \qquad \text{for } \theta\le\theta_M \tag{A4a}$$

$$F=-0.75 \qquad \text{for } \theta>\theta_M \tag{A4b}$$

and

$$\theta_M=180-\sin^{-1}\left(\frac{1}{M_j}\right)$$

The graph in figure 16 is then entered to obtain values of $\mathrm{SPL}_{sh}-\mathrm{UOL}_{sh}$ and consequently values of SPL_{sh}.

TABLE I. – RECOMMENDED SPECTRA FOR JET MIXING NOISE[a]

Frequency parameter, log S_n	Corrected directivity angle (referred to inlet), $\theta' = \theta(V_j/C_a)^{0.1}$, deg										
	0–110	120	130	140	150	160	170	180	190	200	250
	Normalized sound pressure level, $SPL_n - UOL_n$, dB										
−3.6	−85.0	−90.0	−95.0	−100.0	−100.0	−100.0	−100.0	−90.0	−80.0	−70.0	−60.0
−1.8	−40.5	−40.4	−40.4	−40.3	−40.1	−39.5	−37.5	−36.0	−35.0	−34.0	−33.8
−1.7	−38.0	−37.8	−37.4	−37.1	−37.0	−36.4	−33.5	−33.0	−32.5	−32.0	−32.0
−1.6	−35.6	−35.4	−34.4	−33.8	−33.5	−33.3	−30.0	−30.0	−30.0	−30.0	−31.0
−1.5	−33.3	−33.2	−31.4	−30.3	−30.0	−29.5	−27.0	−27.0	−27.5	−28.0	−30.0
−1.4	−30.9	−30.9	−28.5	−26.8	−26.4	−25.5	−24.5	−25.0	−25.5	−26.0	−31.0
−1.3	−28.6	−28.6	−25.7	−23.4	−23.0	−22.8	−22.5	−23.0	−23.5	−24.0	−32.5
−1.2	−26.2	−26.2	−22.9	−19.8	−19.4	−20.0	−20.5	−21.0	−21.5	−22.0	−34.5
−1.1	−24.0	−24.0	−20.1	−16.2	−16.8	−17.5	−18.5	−19.0	−19.5	−20.0	−36.6
−1.0	−21.8	−21.8	−17.3	−13.2	−14.5	−16.2	−16.5	−17.0	−17.5	−18.5	−38.8
−.9	−19.5	−19.5	−14.7	−11.2	−13.1	−14.7	−15.5	−16.0	−17.0	−19.0	−40.1
−.8	−17.5	−17.4	−13.0	−10.2	−11.0	−13.5	−14.5	−15.5	−17.5	−20.0	−42.5
−.7	−15.9	−15.6	−11.5	−9.5	−9.4	−12.6	−14.0	−16.5	−18.5	−21.0	−45.0
−.6	−14.7	−14.0	−9.7	−8.8	−8.3	−12.0	−14.5	−18.0	−20.0	−22.0	−47.5
−.5	−13.7	−12.4	−9.0	−8.1	−7.7	−11.7	−15.8	−20.0	−21.8	−23.5	−50.0
−.4	−12.8	−11.0	−8.9	−8.4	−8.3	−12.6	−17.9	−22.2	−24.1	−25.9	−52.5
−.3	−12.1	−10.2	−9.1	−8.9	−9.8	−14.5	−20.0	−24.4	−26.4	−28.3	−55.0
−.2	−11.6	−9.9	−9.6	−9.8	−11.6	−16.4	−22.1	−26.6	−28.7	−30.7	−57.5
−.1	−11.3	−10.2	−10.8	−11.3	−13.4	−18.3	−24.2	−28.8	−31.0	−33.1	−60.0
0	−11.1	−10.6	−12.0	−12.9	−15.2	−20.2	−26.3	−31.0	−33.3	−35.5	−62.5
.1	−11.2	−11.1	−13.3	−14.5	−17.0	−22.1	−28.4	−33.2	−35.6	−37.9	−65.0
.2	−11.3	−11.8	−14.6	−16.1	−18.8	−24.0	−30.5	−35.4	−37.9	−40.3	−67.5
.3	−11.7	−12.7	−15.9	−17.7	−20.6	−25.9	−32.6	−37.6	−40.2	−42.7	−70.0
.4	−12.3	−13.7	−17.2	−19.3	−22.4	−27.8	−34.7	−39.8	−42.5	−45.1	−72.5
.5	−13.0	−14.7	−18.5	−20.9	−24.2	−29.7	−36.8	−42.0	−44.8	−47.5	−75.0
.6	−13.7	−15.8	−19.8	−22.5	−26.0	−31.6	−38.9	−44.2	−47.1	−49.9	−77.5
.7	−14.6	−16.9	−21.1	−24.1	−27.8	−33.5	−41.0	−46.4	−49.4	−52.3	−80.0
.8	−15.6	−18.0	−22.4	−25.7	−29.6	−35.4	−43.1	−48.6	−51.7	−54.7	−82.5
.9	−16.7	−19.2	−23.7	−27.3	−31.4	−37.3	−45.2	−50.8	−54.0	−57.1	−85.0
1.0	−17.8	−20.4	−25.0	−28.9	−33.2	−39.2	−47.3	−53.0	−56.3	−59.5	−87.5
1.1	−18.9	−21.6	−26.3	−30.5	−35.0	−41.1	−49.4	−55.2	−58.6	−61.9	−90.0
1.2	−20.1	−22.8	−27.6	−32.1	−36.8	−43.0	−51.5	−57.4	−60.9	−64.3	−92.5
1.3	−21.3	−24.0	−28.9	−33.7	−38.6	−44.9	−53.6	−59.6	−63.2	−66.7	−95.0
1.4	−22.4	−25.2	−30.2	−35.3	−40.4	−46.8	−55.7	−61.8	−65.5	−69.1	−97.5
1.5	−23.6	−26.4	−31.5	−36.9	−42.2	−48.7	−57.8	−64.0	−67.8	−71.5	−100.0
1.6	−24.8	−27.6	−32.8	−38.5	−44.0	−50.6	−59.9	−65.2	−70.1	−73.9	−102.5
1.7	−26.0	−28.8	−34.1	−40.1	−45.8	−52.5	−62.0	−68.4	−72.4	−6.3	−105.0
1.8	−27.2	−30.0	−35.4	−41.7	−47.6	−54.4	−64.1	−70.6	−74.7	−78.7	−107.5
3.6	−48.8	−51.6	−58.8	−70.5	−80.0	−88.6	−101.9	−110.2	−116.1	−121.9	−152.5
OASPL–UOL	0	.1	.5	1.1	.4	−3.2	−5.8	−7.7	−9.0	−10.6	------

[a]From ref. 12.

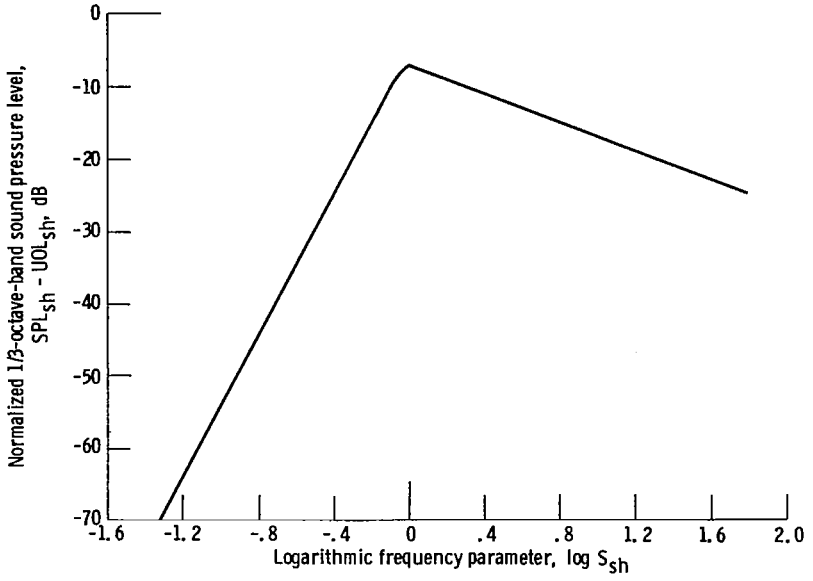

Figure 16. – Recommended 1/3-octave-band spectrum for shock noise. (From ref. 12.)

As mentioned previously, SPL_n and SPL_{sh} are added antilogarithmically to obtain a final sound pressure level for the frequency, angle, and flow conditions of interest.

Calculation of Ideal Thrust

Ideal thrust t_{id} for a TAS configuration was calculated from the following equations: For subsonic flow from the primary nozzle

$$t_{id} = w_j V_j + w_s V_s \tag{A5}$$

For supersonic flow from the primary nozzle,

$$t_{id} = w_j C_j + A_j(P_e - P_a) + w_s V_s \tag{A6}$$

where

C_j primary-nozzle sonic velocity
A_j primary-nozzle exit flow area
P_e static pressure at primary-nozzle exit plane, $(PR_j/1.89) \times P_a$
P_a atmospheric pressure

Appendix B
Symbols

A	area, cm^2
C	speed of sound, m/sec
D	diameter, cm
F	function relation (eq. (A4a))
f	1/3-octave-band center frequency, Hz
h	annular gap width (fig. 3), cm
M	Mach number
OASPL	overall sound pressure level, dB (re 20 $\mu N/cm^2$)
P	pressure, Pa
R	distance from center of nozzle exit plane to microphone, m
S	frequency parameter
SPL	sound pressure level, dB re 10 $\mu N/m^2$
T	total temperature, K
t	thrust, N
UOL	predicted overall sound pressure level uncorrected for refraction, dB (re 20 $\mu N/m^2$)
V	velocity, m/sec
w	weight flow, kg/sec
ρ	density, kg/m^3
θ	directivity angle (measured from nozzle inlet centered on nozzle exit)
θ'	effective directivity angle (eq. (A2b))
θ_M	Mach angle (eq. (A4b))
ω	density exponent (eq. (A2a))

Subscripts:

a	ambient
e	nozzle exit
id	ideal
ISA	international standard atmosphere (288 K and 101.3 kN/m^2
j	primary propulsion stream nozzle
m	mixed flow conditions (e.g., $T_m=(w_jT_j+w_sT_s)/(w_j+w_s)$
n	jet exhaust mixing noise
s	shield stream or secondary nozzle
sh	shock noise
t	total
1	inner nozzle
2	outer nozzle

References

1. Goodykoontz, J.: Effect of Semi-Annular Thermal Acoustic Shield on Jet Exhaust Noise. NASA TM-81615, 1980.
2. Weber, R. J.: Aeropropulsion in Year 2000. NASA TM-81416, 1980.
3. O'Keefe, J. V.; Mangiarotty, R. A.; and Pickup, N.: Current Problems and the Future in Advanced Supersonic Transport Noise. AIAA Paper 80-1056, June 1980.
4. Fishbach, L. H.; et al.: NASA Research in Supersonic Propulsion—A Decade of Progress. NASA TM-82862, 1982.
5. Pickup, N.; Mangiarotty, R. A.; and O'Keefe, J. V.: Tests of a Thermal Acoustic Shield with a Supersonic Jet. AIAA Paper 81-2021, Oct. 1981.
6. Wong, R. L. M.; Richarz, W. G.; and Ribner, H. S.: Shielding Concepts for Jet Noise. AIAA Paper 81-2020, Oct. 1981.
7. Yu, J. C.; and Fratello, D. J.: Measurement of Acoustic Shielding by a Turbulent Jet. AIAA Paper 81-2019, Oct. 1981.
8. Vijayaraghavan, A.; and Parathasarathy, S. P.: Noise Shielding by a Hot Subsonic Jet. AIAA Paper 81-2018, Oct. 1981.
9. Gerhold, C. H.: Analytical Model of Jet Shielding. AIAA Paper 82-0051, Jan. 1982.
10. Goldstein, M. E.: High Frequency Sound Emission from Moving Point Multipole Sources Embedded in Arbitrary Transversely Sheared Mean Flows. J. Sound Vib., vol. 80, no. 4, 1982, pp. 499-522.
11. Tanna, H. K.; and Morris, P. J.: The Noise From Normal-Velocity-Profile Coannular Jets. AIAA Paper 81-1992, Oct. 1981.
12. Stone, J. R.; Groesbeck, D. E.; and Zola, C. L.: Conventional Profile Coaxial Jet Noise Prediction. AIAA J., vol. 21, no. 3., Mar. 1983, pp. 336-342.
13. Goodykoontz, J. H.; and Stone, J. R.: Experimental Study of Coaxial Nozzle Exhaust Noise. AIAA Paper 79-0631, Mar. 1979.
14. Shields, F. D.; and Bass, H. E.: Atmospheric Absorption of High Frequency Noise and Application to Fractional-Octave Bands. NASA CR-2760, 1977.
15. Mani, R.; et al.: High Velocity Jet Noise Source Location and Reduction, Task 2, Theoretical Developments and Basic Experiments. R78AEG323, FAA-RD-76-79-2, General Electric Co., May 1978. (AD-A094291.)
16. von Glahn, U. H.: Acoustic Considerations of Flight Effects on Jet Noise Suppressor Nozzles. AIAA Paper 80-0164, Jan. 1980.

1. Report No.	2. Government Accession No.	3. Recipient's Catalog No.
NASA TP-2259		

4. Title and Subtitle	5. Report Date
Fluid Shielding of High-Velocity Jet Noise	January 1984
	6. Performing Organization Code 505-31-32

7. Author(s)	8. Performing Organization Report No.
Jack H. Goodykoontz	E-1705
	10. Work Unit No.

9. Performing Organization Name and Address	11. Contract or Grant No.
National Aeronautics and Space Administration Lewis Research Center Cleveland, Ohio 44135	13. Type of Report and Period Covered Technical Paper
12. Sponsoring Agency Name and Address	14. Sponsoring Agency Code
National Aeronautics and Space Administration Washington, D.C. 20546	

15. Supplementary Notes

16. Abstract

Experimental noise data for a nozzle exhaust system incorporating a thermal acoustic shield (TAS) are presented to show the effect of changes in geometric and flow parameters on attenuation of high-velocity jet exhaust noise in the flyover plane. The results are presented for a 10.00-cm-diameter primary conical nozzle with a TAS configuration consisting of a 2.59- or 5.07-cm-wide annular gap. Shield-stream exhaust velocity was varied from 157 to 248 m/sec to investigate the effect of velocity ratio. The results showed that increasing the annular gap width increases attenuation of high-frequency noise when comparisons are made on the same ideal thrust basis. Varying the velocity ratio had a minor effect on the noise characteristics of the nozzles investigated.

17. Key Words (Suggested by Author(s))	18. Distribution Statement
Jet noise Noise shielding	Unclassified - unlimited STAR Category 71

19. Security Classif. (of this report)	20. Security Classif. (of this page)	21. No. of pages	22. Price*
Unclassified	Unclassified	21	A02

*For sale by the National Technical Information Service, Springfield, Virginia 22161

NASA-Langley, 1984

6 1 IU,H, 831219 S00903DS
DEPT OF THE AIR FORCE
AF WEAPONS LABORATORY
ATTN: TECHNICAL LIBRARY (SUL)
KIRTLAND AFB NM 87117